Wannier-Stark localization in InAs/(GaIn)Sb superlattice diodes

L. Bürkle,* F. Fuchs,† E. Ahlswede,‡ W. Pletschen, and J. Schmitz
Fraunhofer-Institut für Angewandte Festkörperphysik (IAF), Tullastraße 72, D-79108 Freiburg, Germany
(Received 16 January 2001; published 22 June 2001)

We present experimental evidence for the formation of localized Wannier-Stark states in the depletion region of low band-gap InAs/(GaIn)Sb superlattice (SL) infrared photodiodes. In the photocurrent spectra of reverse-biased photodiodes, maxima are observed, that spectrally shift when the strength of the electric field in the depletion region of the diode is changed. Taking into account the spatially indirect type-II nature of interband transitions in InAs/(GaIn)Sb SL's, the spectral positions of the observed maxima can be explained in the framework of localized Wannier-Stark states. Besides photocurrent spectra, the current-voltage (I-V) characteristics of the diodes were investigated. In the reverse-bias regime dominated by Zener tunneling the differential resistance of the diodes reveals an oscillatory behavior. These oscillations are due to a resonant enhancement of the Zener tunneling current by Wannier-Stark states in the depletion region of the SL diode. A model is presented that quantitatively describes the occurrence of the oscillations in the I-V curves. In addition, the influence of a magnetic field on the Wannier-Stark oscillations in the Zener current was investigated. While the period of the oscillations in the I-V curves is conserved, the resonances are shifted, reflecting the energy shift introduced in the Wannier-Stark states by the magnetic field. This voltage shift exhibits a strong dependence on the magnetic-field orientation.

DOI: 10.1103/PhysRevB.64.045315 PACS number(s): 73.40.Gk, 73.40.Kp, 73.50.Pz, 71.70.Ej

I. INTRODUCTION

In a superlattice (SL) consisting of a periodic repetition of quantum wells separated by narrow potential barriers, resonant coupling between individual quantum-well states leads to the formation of three-dimensional mini bands.[1] By applying an electric field F along the SL-growth axis the mini band breaks up into Stark states. At intermediate electric fields the wave functions still extend over several quantum wells, giving rise to interwell Stark transitions.[2] Various experimental techniques such as photocurrent and photoluminescence spectroscopy were employed to investigate transitions between Wannier-Stark states. Recently, the interaction between Zener tunneling and Stark localization was studied theoretically,[3] and the formation of Wannier-Stark resonances in the Zener current of GaAs/AlGaAs SL diodes was experimentally confirmed.[4]

In recent years antimonide-based heterostructures have attracted significant interest, in particular, in the field of optoelectronic devices operating in the mid and far infrared spectral range. In particular, InAs/(GaIn)Sb SL's are well suited for the fabrication of high-performance photodetectors for the 8–12 μm wavelength region[5,6] as well as lasers operating in the midinfrared.[7,8] Such SL's show a broken-gap type-II band alignment with the conduction-band edge of InAs being lower in energy than the (GaIn)Sb valence-band edge. For short-period SL's with sufficiently thin individual layers, confinement and strain effects result in an effective band gap, which is tunable between zero and about 0.3 eV.[9] The thickness of the individual layers in the SL's used for IR photodiodes is typically of the order of 10 atomic monolayers (ML), leading to strong electronic coupling between the adjacent wells. The electron wave function is centered in the InAs layers, but strongly delocalized with a mini-band width typically exceeding 100 meV.[10] However, the type-II character of the system remains due to the localization of heavy hole (HH) states in the (GaIn)Sb layers.

Recent advances in the growth and processing of InAs/(GaIn)Sb SL's on GaSb substrates have led to a high enough material and device quality[6,11] that Wannier-Stark localization can now be studied in this narrow band-gap type-II SL system, using SL photodiodes optimized for mid-IR detection. Here we report the observation of Stark transitions in the photocurrent spectra of reverse-biased photodiodes, which are quantitatively explained by taking into account the type-II character of interband transitions in the SL. Besides optical measurements, we investigated the current-voltage (I-V) characteristics of the photodiodes. The reverse-bias branch of low-gap photodiodes ($E_g \leqslant 0.2$ eV) is dominated by both Zener and defect-assisted tunneling currents. However, with increasing material quality the contribution of defect-assisted tunneling currents reduces and Zener tunneling currents can be observed even at small reverse bias. The I-V curves of the diodes reveal an oscillatory structure in the Zener tunneling current. These oscillations are due to an alignment of Stark states in the conduction band with the top of the valence band that leads to an enhancement of the Zener tunneling current across the depletion region. A model is presented that quantitatively explains the voltage dependence of the oscillations in the I-V curves. In addition, we studied the modification of the Stark localization by a magnetic field oriented parallel or perpendicular to the internal electric field of the diodes. By applying a magnetic field the voltage dependence of the tunneling resonances is shifted, while the period of the oscillations is conserved. We find that the change in energy of the Stark states caused by the magnetic field directly translates into a voltage shift of the oscillations in the I-V curve. However, in contrast to the parallel-field configuration for crossed fields, a strong damping of the tunneling resonances is observed.

 ©2001 The American Physical Society

II. THEORY

A. Optical transitions between Wannier-Stark states

In a SL consisting of a periodic repetition of quantum wells separated by narrow potential barriers, resonant coupling between individual quantum-well states leads to the formation of three-dimensional mini bands. When an electric field F is applied parallel to the growth direction of the SL, adjacent quantum wells are misaligned by an energy eFd_{SL}, where e is the electron charge and d_{SL} is the SL period, and the coupling between the wave functions of individual quantum wells is reduced. As the electric field increases, the carriers in the SL become more and more localized and, thus, the three-dimensional (3D) nature of the mini bands is continuously reduced to quasi-2D Stark states.

At intermediate electric fields the wave functions still extend over several quantum wells giving rise to interwell Stark transitions between heavy- or light- (LH) hole and electron levels whose wave functions are centered in different quantum wells. In a type-I SL the transition energies are given by[2]

$$E_m = E_0 + meFd_{SL}, \quad m = 0, \pm 1, \pm 2, \ldots, \tag{1}$$

where E_0 is the energy of the intrawell transition and m denotes the Stark index. In the limit of a high electric field $F \gg \Delta/ed_{SL}$, where Δ is the mini-band width, the wave functions are completely localized in individual wells, and only intrawell transitions can occur. In contrast to type-I SL's, interband transitions in a type-II SL are spatially indirect, and therefore the Stark indices assume the values $m = \pm 1/2, \pm 3/2, \pm 5/2, \ldots$.

B. Wannier-Stark localization in a magnetic field

The influence of an additional magnetic field B upon quantization effects in the SL strongly depends on the magnetic-field orientation. Neglecting the excitonic interaction and assuming parabolic bands, the Hamiltonian for a magnetic field parallel to the growth axis $(B \| z)$ of the SL decouples into two independent terms: one describing the motion along the growth axis due to the SL potential and the electric field, and one describing the in-plane motion in the presence of the magnetic field. Then each of the Stark transitions is split into a series of Landau transitions,[12]

$$E_{n,m} = E_0 + \left(n + \frac{1}{2}\right)\hbar\omega_c + meFd_{SL}, \tag{2}$$

where n is the Landau-level index and $\omega_c = eB/m^*$ is the cyclotron frequency.

However, when the magnetic field is applied perpendicular to the growth axis $(B \perp z)$ the situation is different, as in this case the Hamiltonian describing the motion along the growth axis includes an additional potential $m^*\omega_c^2 z^2/2$, which is quadratically magnetic-field dependent.[13] Since the magnetic field tends to localize the electron motion to cyclotron orbits in the same plane as that of the SL-confinement potential there is a competition of electric-field-induced and magnetic-field-induced localization. Depending on the relative strengths of the electric and the magnetic field, three different regions can be distinguished. At small magnetic fields the electric-field-induced localization prevails and the energy of the Stark states exhibits a parabolic dependence on the magnetic field. This energy dependence is due to the diamagnetic shift and is proportional to $m^2 d_{SL}^2 B^2$, where m is the Stark index.[14] Moreover, the energy levels show a dispersion as a function of position of the cyclotron orbit center in the quantum well, which increases with magnetic field.[12,13] In a second region both effects become comparable and the description in terms of Stark states breaks down. At high magnetic fields, the magnetic-field-induced localization dominates and the quantization energies can be described in terms of Landau states $(E_n \propto B)$.

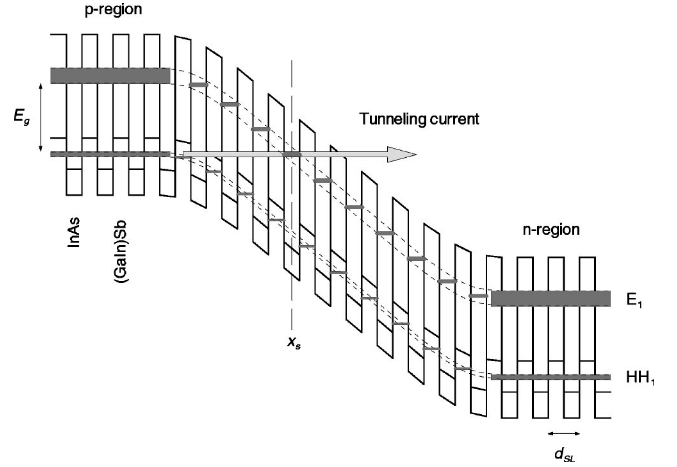

FIG. 1. Schematic illustration for the occurrence of Wannier-Stark oscillations in the Zener-tunneling current of an InAs/(GaIn)Sb SL diode.

C. Wannier-Stark resonances in the Zener tunneling current

When a high reverse bias is applied to a p-n junction, electrons can tunnel from the top of the valence band of the p region through the band gap into the conduction band of the n region. This effect is known as Zener tunneling and results in an exponential current-voltage dependence.[15,16] Di Carlo *et al.* theoretically studied the interaction between Zener tunneling and Stark localization and predicted the occurrence of Wannier-Stark oscillations in the Zener tunneling current of SL diodes.[3] Figure 1 shows a schematic explanation for such Wannier-Stark oscillations in a InAs/(GaIn)Sb SL diode. When a strong reverse bias is applied to the p-n junction of a SL diode, localized Wannier-Stark states form out of the mini band due to the high electric field in the depletion region. Each time when a Stark state becomes energetically aligned with the first heavy-hole (HH_1) valence band, the tunneling current originating from the valence-band edge at the boundary of the depletion layer in the p region into the continuum states of the n region of the SL diode is resonantly enhanced. As the reverse bias is increased, energetically higher-lying Stark states whose wave functions are centered in adjacent quantum wells can be reached by the tunneling electrons leading to an oscillatory behavior in the Zener tunneling current.[4]

TABLE I. Properties of the investigated SL diode structures.

	SL period d_{SL}	Energy gap E_g	Acceptor conc. near the p-n junction N_A	Donor conc. near the p-n junction N_D	Depletion widths d_p	Depletion widths d_n
Sample A	6.51 nm	155 meV	6×10^{16} cm^{-3}	2×10^{16} cm^{-3}	33 nm	98 nm
Sample B	4.8 nm	140 meV	2.3×10^{16} cm^{-3}	1.0×10^{16} cm^{-3}	56 nm	128 nm

In the Appendix it is shown that the voltages $U_S^{(i)}$, at which Stark resonances in the tunneling current occur, follow a recursive relationship

$$U_S^{(i)}=U_S^{(i-1)}-U_{bi}\left(\frac{d_{SL}^2}{d_p^2}+\frac{2d_{SL}}{d_p}\sqrt{1-\frac{U_S^{(i-1)}}{U_{bi}}}\right), \qquad (3)$$

where

$$d_p=\sqrt{\frac{2\epsilon U_{bi}}{e}\frac{N_D/N_A}{N_A+N_D}}, \qquad (4)$$

is the p depletion-layer width at equilibrium, and U_{bi} denotes the builtin potential of the p-n junction. The oscillation period $\Delta U_S=U_S^{(i)}-U_S^{(i-1)}$ of the Wannier-Stark resonances increases with applied reverse bias. Since $d_{SL}\ll d_p$, the oscillation period ΔU_S depends almost linearly on the SL period, while it is reciprocally dependent on the zero-bias p depletion-layer width d_p, which in turn is dependent on the doping profile in the diode.

III. EXPERIMENTAL RESULTS AND DISCUSSION

In Sec. III A we investigate the photocurrent spectra of an InAs/(GaIn)Sb SL infrared photodiode under the influence of an applied reverse bias. The results of these electro-optical studies give clear evidence that localized Wannier-Stark states form in the depletion region of the SL diodes. In Sec. III B, measurements of the current-voltage characteristics of the photodiodes are presented. In the Zener-current regime the differential resistance of the diodes reveals an oscillatory structure that can be explained by a resonant enhancement of the tunneling currents by Stark states in the depletion region of the SL diode. In Sec. III C the influence of a magnetic field oriented parallel and perpendicular to the SL-layer plane on the Wannier-Stark resonances in the Zener current of the photodiodes is investigated.

The SL-photodiode structures used in our study were grown by solid-source molecular-beam epitaxy (MBE) at substrate temperatures of 420 °C on undoped (100) GaSb substrates. Overall strain compensation of the SL stack was achieved by appropriate interface engineering. While for growth on GaSb substrates the smaller lattice constant of InAs is effectively compensated by the larger lattice parameter of $Ga_{1-x}In_xSb$ $(0.1\leq x\leq 0.3)$, with the detailed strain balance depending on the InAs to (GaIn)Sb layer-thickness ratio, the interfaces across which both the group-III and group-V atoms change have to be dealt with separately. For InAs/(GaIn)Sb SL's two types of interfaces with either Ga-As or In-Sb interface bonds can be realized, which differ strongly in interface bond length and strain introduced into the SL stack. Best strain compensation and material quality was achieved by growing the layers with alternating GaAs-like and InSb-like interfaces, terminating each individual layer with its group-V element and starting the following layer with a ML of the respective group-III element.[17–19]

Both effects, the Stark transitions in the photocurrent spectra and the Wannier-Stark resonances in the Zener current were observed more or less pronounced in a large number of samples. However, in this paper we will restrict our analysis to two samples designated with the letters A and B (Table I). The epitaxial-layer sequence of the investigated photodiodes consists of 150 periods of the $InAs/Ga_{1-x}In_xSb$ SL sandwiched between GaSb:Be and InAs:Si contact layers. The SL in sample A consists of 12-ML InAs alternated with 10-ML $Ga_{0.85}In_{0.15}Sb$, whereas the SL in sample B is composed of 10-ML InAs and 5-ML $Ga_{0.75}In_{0.25}Sb$. The SL's in both samples are intentionally doped to form a p-n homojunction diode structure. The doping profile of sample A consists of 85 periods of a moderately p-doped region $(\sim6\times10^{16}$ cm$^{-3})$, followed by 15 periods of a nominally undoped but residual n-type region $(\sim2\times10^{16}$ cm$^{-3})$ and 50 periods of a highly n-doped region $(\sim1\times10^{18}$ cm$^{-3})$. In sample B the first 60 periods of the SL are highly p-doped $(\sim5.7\times10^{16}$ cm$^{-3})$, followed by 30 periods of a moderately p-doped region $(\sim2.3\times10^{16}$ cm$^{-3})$, 40 periods of a nominally undoped but residual n-type region $(\sim1\times10^{16}$ cm$^{3})$, and 20 periods of a highly n-doped region $(\sim1.8\times10^{17}$ cm$^{-3})$. More details of the MBE growth and processing of the photodiodes can be found elsewhere.[20]

Structural properties of the samples such as SL period, residual lattice mismatch, and overall SL thickness were assessed by high-resolution x-ray diffraction (HRXRD). The SL in sample A has a period of 6.51 nm, while the SL in sample B exhibits a period of 4.8 nm. The lattice mismatch $\Delta a/a$ of both samples lies well below 1×10^{-3}. In addition, interference oscillations from the SL stack are observed in the diffraction pattern indicating an excellent material quality. The SL band gap as determined from photoresponse measurements is 155 meV for sample A and 140 meV for sample B. The differential resistance at zero bias, R_0A, of both diodes exhibits diffusion-limited performance down to 100 K and is limited by generation-recombination (GR) currents at lower temperatures.[11] The suppression of trap-assisted tunneling is a prerequisite for the observation of Zener currents down to relatively small reverse biases in narrow-gap photodiodes.

A. Optical transitions between Wannier-Stark states

The formation of localized Wannier-Stark states in the depletion region of InAs/(GaIn)Sb SL photodiodes was in-

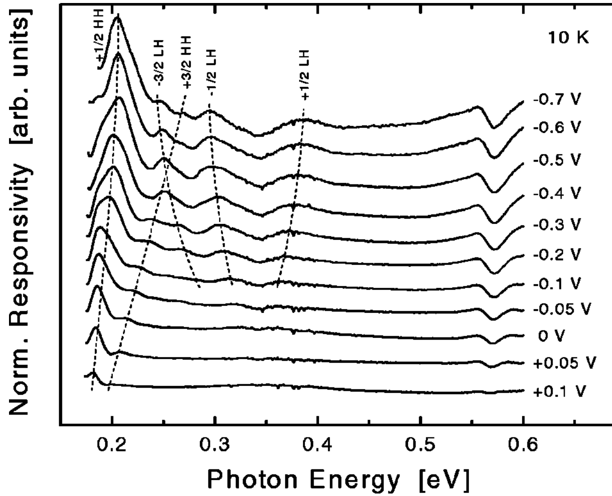

FIG. 2. Normalized photoresponse of a InAs/(GaIn)Sb superlattice diode (sample A) as a function of applied dc voltage.

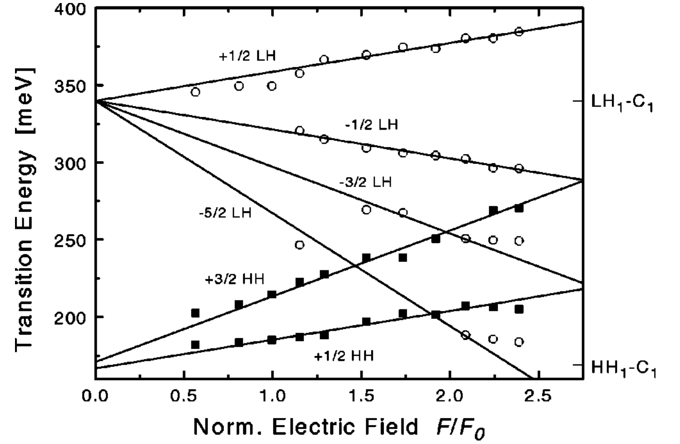

FIG. 3. Observed Wannier-Stark transitions as a function of the normalized electric field (sample A) in the depletion region. Transitions from the first heavy-hole band are marked by solid squares and transitions originating from the first light-hole band by open circles. The labels indicate the Stark-transition indices.

vestigated by measuring photocurrent spectra of the devices as a function of an applied dc voltage. Since the electric field in the diodes extends only over the relatively small depletion region, whereas the whole SL contributes to the photo response, the contribution of Stark transitions to the overall photosignal of the diodes is quite small. Therefore, the measured spectra were normalized to a reference spectrum taken with an applied bias of $U \approx U_{bi}$, at which the electric field in the diodes vanishes and the diodes are in flat-band condition. During the measurement the samples were mounted on the cold finger of a cryostat and the sample temperature was kept at 10 K. The photoresponse spectra were measured using a Fourier Transform IR (FTIR) spectrometer.

Figure 2 shows the normalized photocurrent spectra of sample A for different applied voltages in an energy range between 165 and 600 meV. The spectral response was normalized to a photocurrent spectrum measured at $U = +0.12$ V. In the normalized spectra a series of peaks can be observed that undergo significant energy shifts with increasing reverse bias as indicated in the figure by the dashed lines. These peaks arise from interband transitions between Wannier-Stark states that are localized in adjacent quantum wells in the depletion region of the diode and whose energy difference is determined by the electric field. Based on the results of a 8×8 envelope-function approximation (EFA) model,[10] the observed peaks can be assigned to transitions into Stark states of the first conduction band (C_1) of the SL originating from both, the first heavy-hole and the first light-hole (LH_1) bands. The observation of such transitions clearly indicates the formation of localized Wannier-Stark states in the depletion region of the SL diode. Apart from the Stark transitions a spectral signature is observed at 572 meV, which is not shifted in energy by the applied voltage. This spectral feature arises from a transition in the field-free region of the SL diode outside the depletion layer. The energy of the spectral feature can be identified with a HH_1-C_2 interband transition at the boundary of the SL Brillouin zone at $q_z = \pi/d_{SL}$.[10]

The maximum electric field in the depletion region F of the SL diode can be calculated from the applied bias U using the relation

$$F = F_0\sqrt{1-\frac{U}{U_{bi}}}, \tag{5}$$

where the built in voltage of the p-n junction $U_{bi} = 0.148$ V was determined from a simulation of the band alignment in the diode, and where F_0 is the maximum electric field in the depletion region at equilibrium.

In Fig. 3 the energies of the Stark transitions are plotted as a function of the maximum normalized electric field F/F_0 in the depletion region. Transitions originating from the first heavy-hole band are marked by solid squares and transitions originating from the first light-hole band by open circles, and the labels indicate the indices of the Stark transitions. As expected, the Stark transitions exhibit a linear dependence on the normalized electric field F/F_0 in the depletion region of the diode. However, in contrast to type-I SL's, interband transitions in a type-II SL are spatially indirect and therefore the Stark-transition energies are given by

$$E_m = E_0 + meFd_{SL}$$

with the Stark indices

$$m = \pm 1/2, \pm 3/2, \pm 5/2, \ldots, \tag{6}$$

where the zero-field transition energies E_0 of Stark transitions originating from the HH_1 and LH_1 bands of the SL are 169 and 340 meV, respectively. The slopes $med_{SL}F_0$ of the observed Stark transitions are summarized in Table II. From the slopes a maximum zero-bias electric field of $F_0 = (50 \pm 10)$ kV/cm in the depletion region of the diode can be calculated using the SL period $d_{SL} = 6.51$ nm as determined by HRXRD.

TABLE II. Summary of the observed Stark transitions.

Transition	Zero-field transition energy E_0	Stark index m	Slope $med_{SL}F_0$
HH_1-C_1	167 meV	$+1/2$	$+18.7$ meV
	171 meV	$+3/2$	$+42.5$ meV
LH_1-C_1	340 meV	$-5/2$	-72.9 meV
	340 meV	$-3/2$	-42.9 meV
	340 meV	$-1/2$	-18.7 meV
	340 meV	$+1/2$	$+18.7$ meV

B. Wannier-Stark resonances in the Zener-tunneling current

Besides photocurrent spectra, the *I-V* characteristics of the InAs/(GaIn)Sb SL diodes were investigated. The diode *I-V* curves were measured with a HP5145B parameter analyzer. Since the Wannier-Stark resonances are relatively weak, the oscillations in the tunneling current can be better resolved in the differential resistance, which was calculated from the *I-V* data by numerical differentiation. Figure 4 shows the measured differential resistance of SL diodes on sample *A* and *B* as a function of applied bias at 77 K. For both samples Wannier-Stark oscillations in the Zener current can be clearly observed. However, the oscillation period of the sample *A* diode exceeds that of the diode on sample *B* by roughly a factor of 2.5. The oscillations set in at approximately -0.6 V when localized Wannier-Stark states form in the depletion region of the diode, which is the case when the energy separation between Wannier-Stark states is greater than their collision broadening. The oscillations in the tunneling current exhibit a rapid increase in both period and amplitude. The increase in spacing between oscillation peaks with increasing reverse bias reflects the fact that the energy separation between neighboring Stark states increases linearly with the electric field in the depletion layer. On the other hand, the increasing oscillation amplitude can be explained with the increasing localization of Stark states with electric field.

The voltages corresponding to Wannier-Stark oscillation peaks in the differential resistance of the diode from sample B are shown in Fig. 5. Since at high currents the influence of the series resistance R_S on the current-voltage characteristics of the diode is substantial, the plotted voltages were corrected for the voltage drop R_SJ across the series resistance. The value of the series resistance $R_S = 5.25\times10^{-4}\ \Omega\ \mathrm{cm}^2$ was determined from the forward branch of the diode *I-V* characteristic.

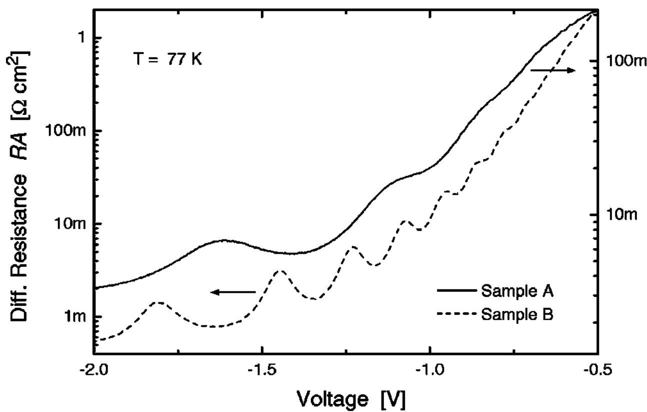

FIG. 4. Differential resistance as a function of applied voltage of an InAs/(GaIn)Sb superlattice diode measured at 77 K. Oscillations in the Zener current can be clearly observed.

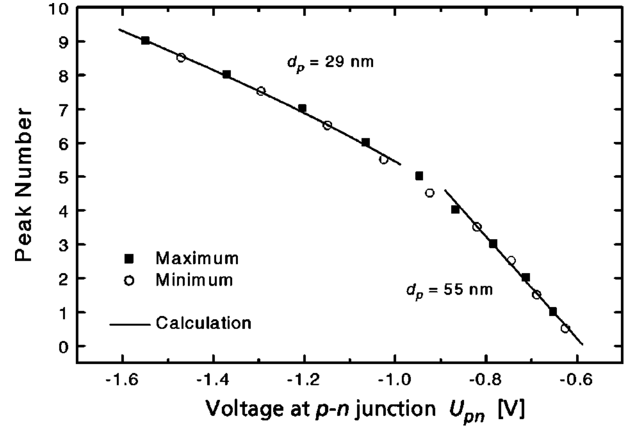

FIG. 5. Voltages at the *p-n* junction of the oscillation peaks in the Zener current (sample *B*). The curves connect the voltages calculated with Eq. (3).

In Fig. 5 two voltage ranges can be distinguished. At small reverse voltages up to approximately -0.8 V the spacing between adjacent maxima ΔU_S is relatively small and lies in a range between 60 and 80 mV. However, at applied reverse biases above -1.0 V the spacing lies between 140 and 180 mV. The occurrence of these two voltage ranges can be explained by the doping profile of the diode. As stated earlier, the diode *p* region consists of a 30-period-wide weakly doped region near the *p-n* junction and a higher-doped region towards the *p* contact. At small reverse biases the depletion layer only extends into the weakly doped *p* region. Because of the low doping the value of d_p is high, and the depletion layer expands rapidly into the weakly doped *p* region with increasing reverse bias. According to Eq. (3), this corresponds to a small spacing between Wannier-Stark oscillations in the tunneling current. At a voltage of approximately -0.9 V the depletion layer reaches the higher-doped *p* region, and from then on expands more slowly with increasing reverse bias. The slower expansion of the depletion region is described by a smaller effective value of d_p. Correspondingly, the Stark states pass the top of the valence band more slowly and, therefore, the spacing between oscillations in the tunneling current increases.

In Fig. 5 the solid curves connect the bias values calculated from the recursive expression of Eq. (3). The calculated curves were fit to the experimental data using the *p*-depletion-layer width at equilibrium d_p and the first voltage of the recursion $U_S^{(1)}$ as fitting parameters. The calculated voltages are in excellent agreement with the experimental data with a maximum deviation of less than 0.5 %. Each of the two voltage ranges was fit with a different d_p value, respectively. For the low-voltage range a value of $d_p = 55$ nm, and for the high-voltage range a value of d_p

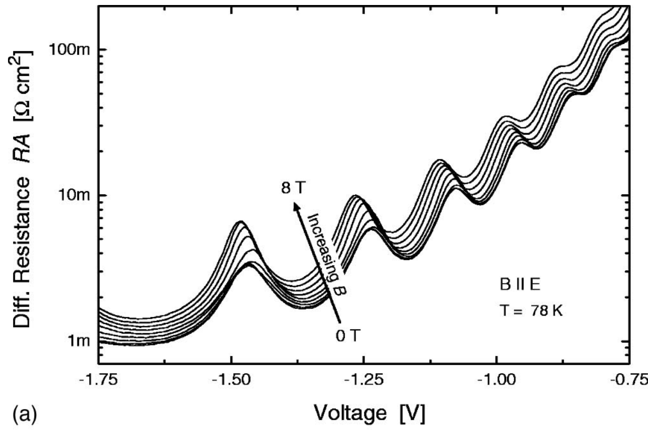

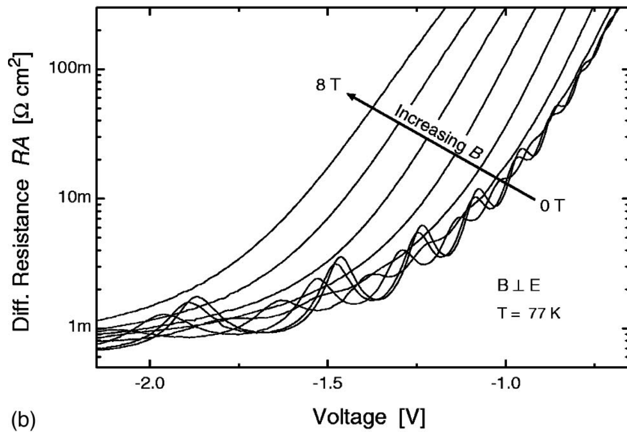

FIG. 6. Wannier-Stark oscillations in the Zener current of a InAs/(GaIn)Sb superlattice diode (sample B) with a magnetic field applied (a) parallel and (b) perpendicular to the electric field in the depletion region.

$=29$ nm was obtained from the fitting procedure. The value of $d_p=55$ nm for the low-voltage regime obtained from the fit is also in good agreement with the p-depletion-layer width $d_p=56$ nm calculated using Eq. (4) and the values in Table I.

According to Eq. (3) the larger oscillation period of the diode from sample A cannot be explained by the larger SL period alone, since this would only increase the spacing between the oscillations by a factor of 1.5. The increase in the oscillation period is a result of both the larger SL period and the different doping profile of that sample. Using Eq. (4) a value of $d_p=33$ nm for the p-depletion-layer width at equilibrium can be calculated for sample A. With this value one obtains a ratio d_{SL}/d_p, which exceeds that of sample B by a factor of 2.3. This value is very close to the increase in the oscillation period experimentally observed in the I-V curves.

C. Wannier-Stark resonances under the influence of a magnetic field

The Wannier-Stark resonances in the Zener current were also investigated with an applied external magnetic field. Figures 6(a) and 6(b) show the differential resistance vs voltage characteristics of the InAs/(GaIn)Sb SL diode on sample

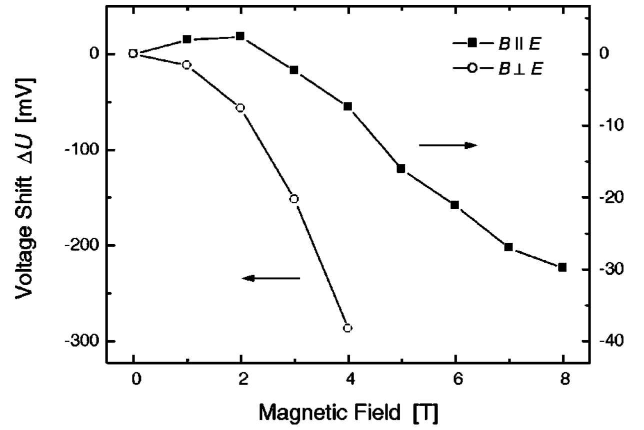

FIG. 7. Shift of the oscillation peak at $U=1.07$ V in the Zener-tunneling current as a function of the applied magnetic field for parallel and crossed electric and magnetic fields.

B with a magnetic field applied parallel and perpendicular to the electric field in the depletion region, respectively. In both cases the magnetic field was varied between $B=0-8$ T in steps of 1 T.

When a magnetic field parallel to the diode current (i.e., perpendicular to the layers of the SL) is applied $(B\|E)$, the Wannier-Stark oscillations in the tunneling current are slightly shifted in the direction of higher reverse biases, and the oscillation peaks become sharpened with increasing field. However, period and amplitude of the oscillation are not influenced by the magnetic field and remain unchanged. In addition, the longitudinal magnetic field decreases the tunneling current (increase in the RA product) by increasing the effective energy gap of the p-n junction due to Landau quantization.[16,21] In Fig. 7 the shift of the oscillation maximum in the differential resistance at $U_S=1.07$ V is plotted as a function of the applied magnetic field. At small fields up to ~ 2 T a small shift of the peaks of about 2 mV in the direction of smaller reverse biases occurs. This effect is even more pronounced for peaks at higher reverse biases and, hence, is attributed to the series resistance of the diode. At magnetic fields exceeding 2 T the peaks are shifted almost linearly with ~ 6 mV/T in the direction of higher reverse biases. The overall shift of the oscillation peaks amounts to 30 mV at 8 T.

In the case of crossed magnetic and electric fields $(B\perp E)$ a much stronger shift of the Wannier-Stark oscillations in the direction of higher reverse biases is observed. At 4 T the overall shift of the oscillation peaks already amounts to 290 mV. Again, the oscillation period is not affected by the magnetic field. However, the oscillation peaks broaden and the amplitude decreases so rapidly with increasing magnetic field, that above 4 T the oscillations in the tunneling current have completely disappeared. Furthermore, the transverse magnetic field strongly decreases the tunneling current (increase in the RA product). This reduction is due to a strong enhancement of the effective tunneling barrier by the additional magnetic potential $m^*\omega_c^2 z^2/2$.[16,21] In Fig. 7 the shift of the maximum in the differential resistance at $U_S=1.07$ V is shown as a function of the applied magnetic field. The volt-

age shift ΔU of the oscillation peaks exhibits a nonlinear behavior according to $\Delta U \propto B^{2.3}$.

For both field orientations, the observed shifts of the oscillation peaks in the direction of higher reverse biases can be explained by a shift of the Stark states to higher energies induced by the magnetic field. If the Stark states are increased in energy due to the magnetic field by an amount ΔE_m, a higher reverse bias $U+\Delta U$ has to be applied to the p-n junction of the diode in order to realign the Stark state with the valence-band edge. Hence, a small energy shift ΔE_m of a Stark state introduces a shift in the Wannier-Stark oscillations ΔU, which is in good approximation proportional to the energy shift: $\Delta U = -\gamma \Delta E_m$, where γ is a proportionality constant.

In the parallel-field orientation ($B \| E$), the increase in energy of the Stark states is due to Landau quantization, and is determined by $\hbar e/2m^* = 2.5$ meV/T, where an in-plane effective electron mass of $m_e^* = 0.0235 m_0$ was used in the calculation.[10] Thus, from the observed shift of -6 mV/T in the oscillation peaks of sample B a value of 2.4 V/eV can be deduced for the proportionality constant γ. On the other hand for crossed fields ($B \perp E$), the diamagnetic shift of the Stark states alone is too small to cause a shift in the Wannier-Stark oscillations as large as that observed in our measurements. The increase in energy of the Stark states is primarily due to the magnetic potential $e^2 B^2 z^2 / 2m^*$ and is, thus, determined by the distance d_T between the initial valence-band state and the Stark state involved in the tunneling process. Both the linear magnetic-field dependence of the Stark states due to Landau quantization for parallel fields ($B \| E$), as well as the quadratic magnetic-field dependence for perpendicular fields ($B \perp E$) as a result of the magnetic potential, directly translate to a shift of the oscillation peaks in the tunneling current. Furthermore, from Eq. (3) it is obvious that a small energy shift ΔE_m of a Stark state and the resulting small shift of the Wannier-Stark oscillation peaks leaves the oscillation period $\Delta U_S = U_S^{(i)} - U_S^{(i-1)}$ nearly unaffected. This explains why no dependence of the oscillation period on the magnetic field was observed in our measurements.

As stated earlier, in the crossed-field orientation ($B \perp E$) both the Stark states and the initial HH_1 valence-band states exhibit a dispersion, which is quadratically dependent on both the position of the cyclotron orbit center in the quantum well and magnetic field.[12,13] Within this framework the disappearance of the Wannier-Stark oscillations in the Zener current under the influence of a perpendicular magnetic field [Fig. 6(b)] can be explained as follows. At magnetic fields smaller than a critical value, oscillations in the Zener tunneling current can be observed. As the reverse bias at the p-n junction is increased, the dispersion curves of the Stark states move downward in energy past the dispersion curve of the initial HH_1 state. Each time the dispersion curve of a Stark state overlaps in energy with the initial-state dispersion curve, the Zener current is resonantly enhanced (Fig. 1). However, when the initial-state dispersion curve lies between two dispersion curves of Stark states from adjacent quantum wells no resonant enhancement is possible, and the tunneling current reaches a minimum (maximum in the RA product). Hence, the oscillations in the Zener current occur because there is a voltage range for which there are no allowed Stark states in the depletion region of the diode that can resonantly enhance the tunneling current. When the magnetic field exceeds a critical value the dispersion is so large that at any diode voltage the initial-state dispersion curve intersects in energy with the dispersion curves of either the first or second or even both Stark states. In this case the Zener current is resonantly enhanced independent of the applied diode voltage and no oscillations in the Zener current can be observed. The critical magnetic field B_c depends on the energy separation between Stark states from adjacent quantum wells eFd_{SL} and, thus, from the electric field in the depletion region of the diode. This explains why the quenching of Wannier-Stark oscillations at smaller reverse biases (i.e., lower electric fields) sets in for lower magnetic fields [Fig. 6(b)].

IV. SUMMARY AND CONCLUSIONS

We presented a comprehensive study of Wannier-Stark localization effects in narrow band gap InAs/(GaIn)Sb SL's. We observed transitions between Wannier-Stark states in the photocurrent spectra of biased InAs/(GaIn)Sb SL photodiodes. The observation of such transitions clearly indicates the formation of localized Wannier-Stark states in the depletion region of the SL diode. Besides photocurrent spectra, the I-V characteristics of the diodes were investigated. In the reverse-bias regime dominated by Zener tunneling, the differential resistance of the diodes revealed an oscillatory structure. These oscillations can be explained by a resonant enhancement of the Zener tunneling current by Stark states in the depletion region of the SL diode. A model was presented that quantitatively describes the occurrence of the oscillations in the I-V curves. Finally, the influence of a magnetic field oriented parallel and perpendicular to the SL layer plane on the Wannier-Stark resonances in the Zener current of the photodiodes was investigated.

ACKNOWLEDGMENTS

The authors would like to thank J. Wagner for helpful discussions, N. Herres and H. Güllich for x-ray analyses, and K. Schwarz and J. Schleife for valuable technical assistance. Continuous support and encouragement by P. Koidl and G. Weimann, and the financial support by the Bundesministerium für Verteidigung are gratefully acknowledged.

APPENDIX

A quantitative description of the Wannier-Stark oscillations in the Zener-tunneling current can be made in the Schottky model of the depletion region of a p-n junction. Let us consider a p-n junction at $x=0$ with the p region extending in the negative and the n region extending in the positive x direction. The potential in the diode is then given by

$$\phi(U,x)=\begin{cases} -\frac{F_0 d_p}{2}\left(1-\frac{U}{U_{bi}}\right), & x\leqslant -d_p\sqrt{1-\frac{U}{U_{bi}}} \\ F_0\left(\frac{x^2}{2d_p}+x\sqrt{1-\frac{U}{U_{bi}}}\right), & -d_p\sqrt{1-\frac{U}{U_{bi}}}<x\leqslant 0 \\ F_0\left(-\frac{x^2}{2\,d_n}+x\sqrt{1-\frac{U}{U_{bi}}}\right), & 0<x<d_n\sqrt{1-\frac{U}{U_{bi}}} \\ \frac{F_0 d_n}{2}\left(1-\frac{U}{U_{bi}}\right), & x\geqslant d_n\sqrt{1-\frac{U}{U_{bi}}}, \end{cases} \tag{A1}$$

where

$$d_n=\sqrt{\frac{2\epsilon U_{bi}}{e}\frac{N_A/N_D}{N_A+N_D}} \tag{A2}$$

$$d_p=\sqrt{\frac{2\epsilon U_{bi}}{e}\frac{N_D/N_A}{N_A+N_D}}, \tag{A3}$$

are the widths of the depletion layers in the n and p regions at equilibrium, respectively. The electric field in the depletion region increases linearly towards the p-n junction, where it reaches its maximum value $F_0=2U_{bi}/(d_n+d_p)$. When a bias U is applied to the p-n junction both the maximum electric field and the width of the depletion region change by the factor $(1-U/U_{bi})^{1/2}$. Hence, the gradient of the electric field $\partial F/\partial x$ is independent of the diode voltage U.

When a high reverse bias is applied to a p-n junction the conduction band on the n side and the valence band on the p side overlap on the energy scale and electrons from the top of the valence band of the p region can tunnel through the band gap into the conduction band of the n region. Such tunneling currents increase exponentially with an applied reverse bias, and are also designated as Zener current. Energy and momentum of the electron are conserved in the tunneling process. In the electric field of the depletion region the electron mini band of a SL is quantized into Stark states. The energy of the Stark states is shifted with respect to the miniband edge by an energy δ_e. Each time a Stark state becomes energetically aligned with the top of the valence band, the Zener-tunneling current is resonantly enhanced (Fig. 1). The position $x_S(U)$ in the depletion region, where a Stark state coincides in energy with the valence-band edge of the p region is given by

$$x_S(U)=\sqrt{\frac{2(E_g+\delta_e)d_p}{eF_0}}-d_p\sqrt{1-\frac{U}{U_{bi}}}. \tag{A4}$$

This position is separated by a constant distance d_T [determined by the first term in Eq. (A4)] from the boundary of the p depletion region and, thus, moves away from the p-n junction with increasing reverse bias. For two succeeding Stark resonances in the Zener current the equation

$$x_S(U_S^{(i)})=x_S(U_S^{(i-1)})-d_{SL} \tag{A5}$$

holds, where $U_S^{(i)}$ designates the voltage of the ith Stark resonance. Together with Eq. (A4) one obtains a recursive expression for the voltages of the Stark resonances

$$U_S^{(i)}=U_S^{(i-1)}-U_{bi}\left(\frac{d_{SL}^2}{d_p^2}+\frac{2d_{SL}}{d_p}\sqrt{1-\frac{U_S^{(i-1)}}{U_{bi}}}\right), \tag{A6}$$

which is independent of the energies E_g and δ_e.

*Electronic address: lutz.buerkle@iaf.fhg.de; URL: http://www.iaf.fhg.de/mf/index.htm

†Electronic address: frank.fuchs@iaf.fhg.de

‡Present address: Max-Planck-Institut für Festkörperforschung, Heisenbergstraße 1, 70569 Stuttgart, Germany.

[1] L. Esaki and R. Tsu, IBM J. Res. Dev. **14**, 61 (1970).

[2] E. E. Mendez, F. Agulló-Rueda, and J. M. Hong, Phys. Rev. Lett. **60**, 2426 (1988).

[3] A. Di Carlo, P. Vogl, and W. Pötz, Phys. Rev. B **50**, 8358 (1994).

[4] C. Hamaguchi, M. Yamaguchi, H. Nagasawa, M. Morifuji, A. Di Carlo, P. Vogl, G. Böhm, G. Tränkle, G. Weimann, Y. Nishikawa, and S. Muto, Jpn. J. Appl. Phys., Part 1 **34**, 4519 (1995).

[5] J. L. Johnson, L. A. Samoska, A. C. Gossard, J. L. Merz, M. D. Jack, G. R. Chapman, B. A. Baumgratz, K. Kosai, and S. M. Johnson, J. Appl. Phys. **80**, 1116 (1996).

[6] F. Fuchs, U. Weimar, W. Pletschen, J. Schmitz, E. Ahlswede, M. Walther, J. Wagner, and P. Koidl, Appl. Phys. Lett. **71**, 3251 (1997).

[7] J. R. Meyer, C. A. Hoffman, F. J. Bartoli, and L. R. Ram-Mohan, Appl. Phys. Lett. **67**, 757 (1995).

[8] W. W. Bewley, H. Lee, I. Vurgaftman, R. J. Menna, C. L. Felix, R. U. Martinelli, D. W. Stokes, D. Z. Garbuzov, J. R. Meyer, M. Maiorov, J. C. Connolly, A. R. Sugg, and G. H. Olsen, Appl. Phys. Lett. **76**, 256 (2000).

[9] D. L. Smith and C. Mailhiot, J. Appl. Phys. **62**, 2545 (1987).

[10] F. Fuchs, E. Ahlswede, U. Weimar, W. Pletschen, J. Schmitz, M. Hartung, B. Jager, and F. Szmulowicz, Appl. Phys. Lett. **73**, 3760 (1998).

[11] L. Büurkle, F. Fuchs, R. Kiefer, W. Pletschen, R. E. Sah, and J. Schmitz, in *Infrared Applications of Semiconductors III*, edited by M. O. Manasreh, B. J. H. Stadler, I. Ferguson, and Y.-H.

Zhang, MRS Symposia Proceedings No. 607 (Materials Research Society, Pittsburgh, 2000), p. 84.

[12] A. Alexandrou, E. E. Mendez, and J. M. Hong, Phys. Rev. B **44**, 1934 (1991).

[13] J. C. Maan, in *Magnetic Quantization in Superlattices*, edited by P. Grosse, Festkörperprobleme/Advances in Solid State Physics Vol. 27 (Vieweg, Braunschweig, 1987), p. 137.

[14] A. Alexandrou, M. M. Dignam, E. E. Mendez, J. E. Sipe, and J. M. Hong, Phys. Rev. B **44**, 13 124 (1991).

[15] S. M. Sze, *Physics of Semiconductor Devices* (Wiley, New York, 1981).

[16] U. Weimar, F. Fuchs, E. Ahlswede, J. Schmitz, W. Pletschen, N. Herres, and M. Walther, in *Infrared Applications of Semiconductors II*, edited by S. Sivananthan, M. O. Manasreh, R. H. Miles, and D. L. McDaniel, Jr., MRS Symposia Proceedings No. 484 (Materials Research Society, Pittsburgh, 1998), p. 123.

[17] N. Herres, F. Fuchs, J. Schmitz, K. M. Pavlov, J. Wagner, J. D. Ralston, P. Koidl, C. Gadaleta, and G. Scamarcio, Phys. Rev. B **53**, 15 688 (1996).

[18] J. Wagner, J. Schmitz, F. Fuchs, U. Weimar, N. Herres, G. Tränkle, and P. Koidl, in *Compound Semiconductor Electronics and Photonics*, edited by R. J. Shul *et al.*, MRS Symposia Proceedings No. 421 (Materials Research Society, Pittsburgh, 1996), p. 39.

[19] J. Wagner, J. Schmitz, N. Herres, F. Fuchs, and M. Walther, J. Appl. Phys. **83**, 5452 (1998).

[20] F. Fuchs, U. Weimar, E. Ahlswede, W. Pletschen, J. Schmitz, and M. Walther, Proc. SPIE **3287**, 14 (1998).

[21] V. V. Zav'ialov and V. F. Radantsev, Semicond. Sci. Technol. **9**, 281 (1994).